Dynamic Analysis of A Redundantly Actuated Parallel Manipulator: A Virtual Work Approach

†Hamid D. Taghirad and ‡Meyer Nahon
†Advanced Robotics and Automated Systems (ARAS),
Department of Electrical Engineering,
K.N. Toosi University of Technology.
‡ Center for Intelligent Machines (CIM),
Department of Mechanical Engineering,
McGill University.

Abstract— **In this paper the dynamic analysis of a parallel manipulator is studied in detail. The manipulator architecture is a simplified planar version adopted from the structure of Large Adaptive Reflector (LAR), the Canadian design of next generation giant radio telescopes. This structure uses a parallel redundant manipulator actuated by cables. In this paper first, the governing dynamic equation of motion of such structure is derived using the principle of virtual work. Next, the dynamic equations of the system are used in simulations. In these simulations it is observed that the limb inertial forces contributes only %10 of the dynamical forces required to generate a typical trajectory, and moreover, the total dynamical forces contribute in only %10 of experimentally measured disturbance forces.**

I. Introduction

An international consortium of radio astronomers and engineers have agreed to investigate technologies to build the Square Kilometer Array (SKA), a cm-to-m wave radio telescope for the next generation of investigation into cosmic phenomena [5]. A looming "sensitivity barrier" will prevent current telescopes from making much deeper inroads at these wavelengths, particularly in studies of the early universe. The Canadian proposal for the SKA design consists of an array of 30-50 individual antennas whose signals are combined to yield the resolution of a much larger antenna. Each of these antennas would use the Large Adaptive Reflector (LAR) concept put forward by a group led by the National Research Council of Canada and supported by university and industry collaborators [1]. The LAR design is applicable to telescopes up to several hundred meters in diameter. However, design and construction of a 200-m LAR prototype is pursued by the National Research Council of Canada. Figure 1 is an artist's concept of a complete 200-m diameter LAR installation, which consists of two central components. The first is a 200 m diameter parabolic reflector with a focal length of 500 m, composed of actuated panels supported by the ground. The second component is the receiver package which is supported by a tension structure consisting of multiple long tethers and a helium filled aerostat. With funding from the Canada Foundation for Innovation, a one-third scale prototype of the multi-tethered aerostat subsystem [6] has been designed and implemented in Penticton. It should be noted that even at 1/3 scale, this system is very large, with a footprint of roughly 1 square kilometer.

The challenging problem in this system is the accurately positioning of the feed (receiver) in the presence of disturbances, such as wind turbulence. For the positioning structure of the receiver a redundantly actuated cable-driven parallel manipulators is used [6]. In which, the receiver is moved to various locations on a circular hemisphere and its positioning is controlled by changing the lengths of eight tethers with ground winches. The cable driven macroredundant manipulator used in this design, which is called the Large Cable Mechanism (LCM), is in fact a 6DOF cable driven redundant manipulator. For sufficient coverage of the sky, LCM must be capable of positioning the receiver for a wide range of zenith angles ($0 \leq \theta_z \leq 60°$) and for the full range of azimuth angles ($0 \leq \theta_a \leq 360°$). Since in the design of LCM a redundantly actuated parallel manipulator is used for extreme positioning accuracy, this paper is intended to study the dynamic analysis of such structures in detail. In the LCM structure, a parallel manipulators with six degrees of freedom is used. In contrast to the open-chain manipulator, the analysis of parallel manipulators with such structures inhibits an inherent complexity, due to their closed loop and kinematic constraints. Therefore, in order to keep the analysis complexity at a managing level, while preserving the important analysis elements, a simplified version of the structure is considered in this paper as the basis of the analysis. This structure is composed of a 4RPR mechanisms actuated by cables. In this simplified structure, although a planar version of the mechanisms are considered, the important feature of the original design namely the actuator redundancy for each subsystem and the cable driven structure of the original design are employed.

In contrast to the open-chain serial manipulators, the dynamic modeling of parallel manipulators presents an inherent complexity due to their closed-loop structure and kinematic constraints. Nevertheless, the dynamic modeling is quite important for their control, particularly because parallel manip-

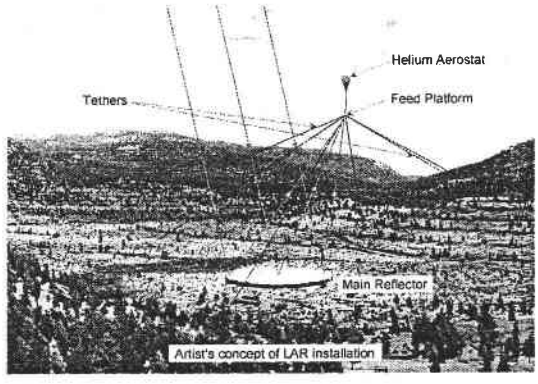

Fig. 1. An artists concept of a complete 200-m diameter LAR installation.

ulators are preferred in applications where precise positioning and good dynamic performance under high load are the prime requirements. In recent years, there has been a great amount of research on the kinematics of parallel manipulators, but works on the dynamics of parallel manipulators are relatively few. Several approaches have been proposed for the dynamic analysis of parallel manipulators. The traditional Newton–Euler formulation is used for the dynamic analysis of general parallel manipulators [4], and also for the Stewart platform, which is the most celebrated parallel manipulator [3]. In this formulation the equation of motion for each limb and the moving platform must be derived, which inevitably leads to a large number of equations and less computational efficiency. On the other hand all the reaction forces can be computed, which is very useful in the design of a parallel manipulator. The Lagrangian formulation eliminates all the unwanted reaction forces at the outset, and it is more efficient, [9]. However, because of the numerous constraints imposed by closed loops of parallel manipulator, deriving explicit equations of motion in terms of a set of independent generalized coordinates becomes a prohibitive task, [7]. A third approach is to use the principle of virtual work, in which the computation of the constraint forces are bypassed, [12]. In this method the inertial forces and moments are computed using the linear and angular accelerations of each of the bodies. Then, the whole manipulator is considered to be in static equilibrium and the principle of virtual work is applied to derive the input force or torque [12]. Since constraint forces and moments do not need to be computed, this approach leads to faster computational algorithms, which is an important advantage for the purposes of control of a manipulator [8]. Among the many control topologies reported in the literature, the dynamics and control of redundantly actuated parallel manipulators has been considered by fewer researchers [2].

Due to the potential attraction of cable driven redundant manipulator structure in the LAR application, a thorough analysis on the kinematics and dynamics of the described redundant parallel manipulator has been developed and some closed loop control topologies are proposed and simulated for this system. In this paper the dynamic analysis of this system is reported. The governing dynamic equation of motion of the redundant manipulator is derived using the principle of virtual work. Furthermore, the dynamic equations of the system is used in two sets of simulations. First, the required actuator torques required to generate a predefined trajectory is computed. It is shown that for a typical trajectory, the limb inertial forces contributes only in %10 of the total dynamical forces. Finally, the total dynamical forces in presence of some experimentally measured disturbance forces are simulated and it is shown that they contribute in only %10 of total external forces.

II. Mechanism Description

The architecture of the planar 4RPR parallel manipulator considered for our studies is shown in figure 2. In this manipulator the moving platform is supported by four limbs of identical kinematic structure. Each limb connects the fixed base to the manipulator moving platform by a revolute joint (R) followed by a prismatic joint (P) and another revolute joint (R). The kinematic structure of a prismatic joint is used to model the elongation of each cable-driven limb. In order to avoid singularities at the central position of the manipulator at each level, the cable-driven limbs are considered to be crossed. Complete singularity analysis of the mechanism is analyzed and presented in [10]. Angular positions of fixed base and moving platform attachment points are given in table I. In this presentation, A_i denote the fixed base points of the limbs. B_i denote point of connection of the limbs on the moving platform, L_i denote the limb lengths, and α_i denotes the limb angles. The position of the center of the moving platform G, is denoted by $G = [x_G, y_G]$, and the orientation of the manipulator moving platform is denoted by ϕ with respect to the fixed coordinate frame.

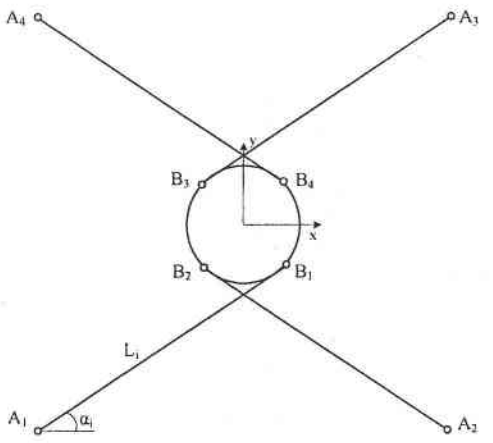

Fig. 2. The schematics of 4RPR mechanism employed for the analysis of LCM structure.

The planar structure used in this analysis, is a simplified version of LCM design. The control objective in the simplified mechanism is to track the position and orientation of the moving platform as desired in presence of disturbance force, such as wind turbulence. The geometric and inertial parameters used in the simulations of the system is adopted from LCM design and is given in Table I, in which M and I denote the mass and the moment of inertia of the moving platform, respectively, ρ denotes the limb density per length.

III. Kinematic Analysis

A. Inverse Kinematics

For inverse kinematic analysis, it is assumed that the position and orientation of the moving platform $\boldsymbol{X} = [x_G, y_G, \phi]^T$ is given and the problem is to find the joint variable of the manipulator, $\boldsymbol{L} = [L_1, L_2, L_3, L_4]^T$. For the purpose of analysis and as it is illustrated in figure 3, a fixed frame $O : xy$ is attached to the fixed base at the point O, the

TABLE I
Geometric And Inertial Parameters of the System

Description	Quantity
R_A: Radius of the fixed points A_i's	$900\ m$
R_B: Radius of the moving points B_i's	$10\ m$
θ_{A_i}: Angle of the fixed points A_i's	$[-\frac{3\pi}{4}, -\frac{\pi}{4}, \frac{\pi}{4}, \frac{3\pi}{4}]$
θ_{B_i}: Angle of the moving points B_i's	$[-\frac{\pi}{4}, -\frac{3\pi}{4}, \frac{3\pi}{4}, \frac{\pi}{4}]$
M: The moving platform mass	$2500\ Kg$
I: The moving platform moment of inertia	$3.5 \times 10^5\ Kg \cdot m^2$
ρ: The limb density per length	$0.215\ Kg/m$

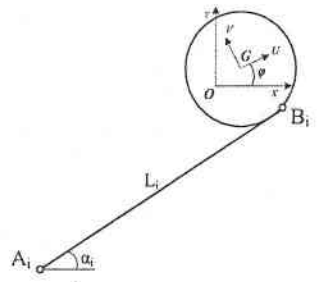

Fig. 3. Kinematic configuration of the manipulator.

center of the base point circle which passes through $A_i's$, and another moving coordinate frame $G : UV$ is attached to the manipulator moving platform at point G. Furthermore, assume that the point A_i lie at the radial distance of R_A from point O, and the point B_i lie at the radial distance of R_B from point G in the xy plane, when the manipulator is at central location.

In order to specify the geometry of the manipulator define θ_{Ai}, θ_{Bi} as the absolute angle of the points A_i and B_i at the central configuration of the manipulator, with respect to the fixed frame O. Let's define the instantaneous orientation angle of B_i's as:

$$\phi_i = \phi + \theta_{Bi}. \tag{1}$$

Therefore, for each limb, $i = 1, 2, \cdots, 4$, the position of the base points, A_i is given by,

$$A_i = [R_A \cos(\theta_{Ai}), R_A \sin(\theta_{Ai})]^T \tag{2}$$

From the geometry of the manipulator as illustrated in figure 3, the loop closure equation for each limb, $i = 1, 2, \cdots, 4$, can be written as,

$$\overrightarrow{A_iG} = \overrightarrow{A_iB_i} + \overrightarrow{B_iG}. \tag{3}$$

Rewriting the vector loop closure component–wise,

$$x_G - x_{Ai} = L_i \cos(\alpha_i) - R_B \cos(\phi_i) \tag{4}$$

$$y_G - y_{Ai} = L_i \sin(\alpha_i) - R_B \sin(\phi_i), \tag{5}$$

in which α_i's are the absolute limb angles. To solve the inverse kinematic problem it is required to eliminate α_i's from the above equation and solve for L_i's. This can be accomplished by reordering the above equation as,

$$L_i \cos(\alpha_i) = x_G - x_{Ai} + R_B \cos(\phi_i) \tag{6}$$

$$L_i \sin(\alpha_i) = y_G - y_{Ai} + R_B \sin(\phi_i), \tag{7}$$

By adding the square of both sides of equations 6 and 7 the limb lengths are uniquely determined.

$$L_i = \left[(x_G - x_{Ai} + R_B \cos(\phi_i))^2 + (y_G - y_{Ai} + R_B \sin(\phi_i))^2\right]^{1/2} \tag{8}$$

Furthermore the limb angles α_i's can be determined from the following equation

$$\alpha_i = \text{atan2}\left[(y_G - y_{Ai} + R_B \sin(\phi_i)), (x_G - x_{Ai} + R_B \cos(\phi_i))\right] \tag{9}$$

Hence, corresponding to each given manipulator location $\boldsymbol{X} = [x_G, y_G, \phi]^T$, there is a unique solution for the limb length L_i's, and limb angles α_i's. Due to the nature of cable-driven actuators, the mechanism experiences no singularities at the boundaries of the workspace, since the actuator lengths can be extended without almost any limits.

B. Jacobian Analysis

Jacobian analysis plays a vital role in the study of robotic manipulators. Jacobian matrix not only reveals the relation between the joint variable velocities $\dot{\boldsymbol{L}}$ and the moving platform velocities $\dot{\boldsymbol{X}}$, it construct the transformation needed to find the actuator forces τ from the forces acting on the moving platform F. On the contrary to the serial manipulators, Jacobian matrix of a parallel manipulator is defined as the transformation matrix that converts the moving platform velocities to the joint variable velocities, i.e.,

$$\dot{\boldsymbol{L}} = J_M \cdot \dot{\boldsymbol{X}} \tag{10}$$

In which, $\dot{\boldsymbol{L}} = [\dot{L}_1, \dot{L}_2, \dot{L}_3, \dot{L}_4]$ is the 4×1 limb velocity vector, and $\dot{\boldsymbol{X}} = [\dot{x}_G, \dot{y}_G, \dot{\phi}]$ is the 3×1 moving platform velocity vector. Therefore, the Jacobian matrix J_M is a non-square 4×3 matrix. In order to obtain the Jacobian matrix, let us differentiate the vector loop equation 3 with respect to time, considering the vector definitions $\hat{S}_i$ and $\overrightarrow{E_i}$ illustrated in figure 4. Hence, for $i = 1, 2, \cdots, 4$:

$$\boldsymbol{v_G} + \dot{\phi}\,(\hat{\boldsymbol{K}} \times \boldsymbol{E_i}) = \dot{L}_i \hat{\boldsymbol{S}}_i + \dot{\alpha}_i L_i\,(\hat{\boldsymbol{K}} \times \hat{\boldsymbol{S}}_i) \tag{11}$$

In which, $\boldsymbol{v_G} = [\dot{x_G}, \dot{y_G}]^T$ is the velocity of the moving platform at point G, and $\hat{\boldsymbol{K}}$ is the unit vector in Z direction of fixed coordinate frame A. In order to eliminate $\dot{\alpha}_i$, dot multiply both sides of equation 11 by $\hat{\boldsymbol{S}}_i$.

$$\hat{\boldsymbol{S}}_i \cdot \boldsymbol{v_G} + \dot{\phi}\,\hat{\boldsymbol{K}}\,(\boldsymbol{E_i} \times \hat{\boldsymbol{S}}_i) = \dot{L}_i \tag{12}$$

Rewriting equation 12 in a matrix form:

$$\dot{L}_i = \left[\; S_{ix} \;\middle|\; S_{iy} \;\middle|\; E_{ix}S_{iy} - E_{iy}S_{ix} \;\right] \cdot \begin{bmatrix} v_{Gx} \\ v_{Gy} \\ \dot{\phi} \end{bmatrix} \tag{13}$$

Using equation 13 for $i = 1, 2, \cdots, 4$ the Jacobian matrix J_M is derived.

$$J_M = \left[\; S_{ix} \;\middle|\; S_{iy} \;\middle|\; E_{ix}S_{iy} - E_{iy}S_{ix} \;\right]_{i=1}^{4} \tag{14}$$

note that the Jacobian matrix J_M is a non-square 3×4 matrix, since the manipulator is a redundant manipulator. In order to get an expression for $\dot{\alpha}_i$, cross multiply both side of 11 by $\hat{\boldsymbol{S}}_i$:

$$\hat{\boldsymbol{S}}_i \times \boldsymbol{v_G} + \dot{\phi}\,(\boldsymbol{E_i} \cdot \hat{\boldsymbol{S}}_i)\,\hat{\boldsymbol{K}} = \dot{\alpha}_i\, L_i\, \hat{\boldsymbol{K}} \tag{15}$$

Rewriting equation 15 in a matrix form:

$$\dot{\alpha}_i = \frac{1}{L_i}\left[\; -S_{iy} \;\middle|\; S_{ix} \;\middle|\; E_{ix}S_{ix} + E_{iy}S_{iy} \;\right] \begin{bmatrix} v_{Gx} \\ v_{Gy} \\ \dot{\phi} \end{bmatrix} \tag{16}$$

Therefore, J_α is defined as the matrix relating the vector of moving platform velocities, $\dot{\boldsymbol{X}} = [\dot{x}_G, \dot{y}_G, \dot{\phi}]$, to the vector of angular velocities of the limbs $\dot{\boldsymbol{\alpha}} = [\dot{\alpha}_1, \dot{\alpha}_2, \dot{\alpha}_3, \dot{\alpha}_4]$ as:

$$\dot{\boldsymbol{\alpha}} = J_\alpha \cdot \dot{\boldsymbol{X}} \tag{17}$$

in which,

$$J_\alpha = \frac{1}{L_i} \cdot \left[\; -S_{iy} \;\middle|\; S_{ix} \;\middle|\; E_{ix}S_{ix} + E_{iy}S_{iy} \;\right]_{i=1}^{4}. \tag{18}$$

C. Acceleration Analysis

Acceleration analysis of the limbs and the moving platform is needed for the Dynamic formulation of a parallel manipulator. In acceleration analysis it is intended to derive expressions for the linear and angular accelerations of the limbs, namely $\ddot{L}_i$ and $\ddot{\alpha}_i$ as a function of the moving platform acceleration $\ddot{\boldsymbol{X}} =$

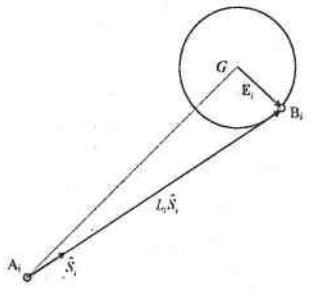

Fig. 4. Vectors definitions for Jacobian derivation of the manipulator.

$[\ddot{x}_G, \ddot{y}_G, \ddot{\phi}]^T$. In order to obtain such relation differentiate the vector loop equation 11 with respect to time, considering the vector definitions $\hat{S}_i$ and $\overrightarrow{E_i}$ illustrated in figure 4, and noting that $\dot{\hat{S}}_i = \dot{\alpha}_i(\hat{K} \times \hat{S}_i)$ and $\dot{E}_i = \dot{\phi}(\hat{K} \times E_i)$. Hence, for $i = 1, 2, \cdots, 4$:

$$\begin{aligned} &a_G + \ddot{\phi}\,(\hat{K} \times E_i) - \dot{\phi}^2 E_i = \ddot{L}_i\,\hat{S}_i + \\ &2\,\dot{L}_i\,\dot{\alpha}_i\,(\hat{K} \times \hat{S}_i) + \ddot{\alpha}_i\,L_i\,(\hat{K} \times \hat{S}_i) - \dot{\alpha}_i^2\,L_i\,\hat{S}_i \end{aligned} \quad (19)$$

In order to eliminate $\ddot{\alpha}_i$ and get an expression for $\ddot{L}_i$, dot multiply both side by $\hat{S}_i$ and reorder into,

$$\ddot{L}_i = a_G \cdot \hat{S}_i + \ddot{\phi}\,\hat{K}(E_i \times \hat{S}_i) - \dot{\phi}^2(E_i \cdot \hat{S}_i) + \dot{\alpha}_i^2\,L_i \quad (20)$$

In order to eliminate $\ddot{L}_i$ and get an expression for $\ddot{\alpha}_i$, cross multiply both side of 19 by $\hat{S}_i$:

$$\hat{S}_i \times a_G + \ddot{\phi}\,(E_i \cdot \hat{S}_i)\,\hat{K} - \dot{\phi}^2(\hat{S}_i \times E_i) = (2\,\dot{L}_i\,\dot{\alpha}_i + \ddot{\alpha}_i\,L_i)\,\hat{K}. \quad (21)$$

This simplifies to,

$$\ddot{\alpha}_i = \tfrac{1}{L_i}\left[\ -S_{iy} \mid S_{ix} \mid E_{ix}S_{ix} + E_{iy}S_{iy}\ \right]\begin{bmatrix} a_{Gx} \\ a_{Gy} \\ \ddot{\phi} \end{bmatrix} - \tfrac{1}{L_i}\left((E_{iy}S_{ix} - E_{ix}S_{iy})\dot{\phi}^2 + 2\,\dot{L}_i\,\dot{\alpha}_i\right). \quad (22)$$

Note that if this equation is written for all four limbs, the first term constitutes J_α, as defined in equation 18. In order to complete the manipulator acceleration analysis it is necessary to derive expressions for the linear accelerations of the center of mass of each limb. Since in the LAR application, the manipulator is cable driven, it is assumed that the center of mass of each limb is located in the middle of the limbs. Denote the velocity and acceleration of the center of mass of the limbs as v_{C_i} and a_{C_i}, respectively. The velocity of the center of mass is composed as the tangential and normal components as,

$$v_{c_i} = \frac{1}{2}\left(\dot{L}_i\hat{S}_i + \dot{\alpha}_i\,L_i\,(\hat{K} \times \hat{S}_i)\right) \quad (23)$$

In order to obtain the relation for acceleration of the center of mass of each limb, differentiate 23 with respect to time.

$$a_{c_i} = \frac{1}{2}\left((\ddot{L}_i - \dot{\alpha}^2\,L_i)\,\hat{S}_i + (\ddot{\alpha}_i\,L_i + 2\,\dot{L}_i\,\dot{\alpha}_i)(\hat{K} \times \hat{S}_i)\right) \quad (24)$$

Note that the velocity and acceleration of the center of mass of the limbs v_{c_i} and a_{c_i} are functions of $\dot{L}_i, \dot{\alpha}_i, \ddot{L}_i$ and $\ddot{\alpha}_i$, whose relation to the manipulator velocity and acceleration $\dot{X}$ and $\ddot{X}$ are given in equations 13, 16, 20 and 22, respectively.

IV. Dynamic Analysis

The most popular approach to derive the dynamics equation of motion of a parallel manipulator is based on the principle of virtual work. In this method the inertial forces and moments are computed using the linear and angular accelerations of each of the bodies. Then, the whole manipulator is considered to be in static equilibrium and the principle of virtual work is applied to derive the input force or torque [12]. Since constraint forces and moments do not need to be computed, this approach leads to faster computational algorithms, which is an important advantage for the purposes of control of a manipulator.

Following d'Alembert's principle, the inertial force and moment on a body are defined as the force and moment exerted at the center of mass of the body and whose magnitude is given respectively by the mass of the link times the acceleration of the center of mass and the inertial tensor of the link times the angular acceleration of the body. These forces and moments are applied in a direction opposite to the direction of the linear and angular accelerations. As it is well known, introducing these virtual forces and moments in the system allows one to consider it as if it were in static equilibrium. If at the static equilibrium a virtual displacement $\delta(\cdot)$ is considered for the system, by application of the principle of the virtual work, one can obtain the input forces of the manipulator. In order to illustrate the method consider the following conventions.

f_i: Resulting external force exerted at the center of mass of link i, excluding the actuator force.

f_i^*: Inertia force exerted at the center of mass of link i.

f_G: Resulting external force exerted at the center of mass of moving platform G.

f_G^*: Inertia force exerted at the center of mass of moving platform G.

n_i: Resulting external moment exerted about the center of mass of link i.

n_i^*: Inertia moment exerted about the center of mass of link i.

n_G: Resulting external moment exerted about the center of mass of moving platform G.

n_G^*: Inertia moment exerted about the center of mass of moving platform G.

F_i: $[f_i, n_i]^T$ the 3D wrench of link i.

F_G: $[f_G, n_G]^T$ the 3D wrench of moving platform on point G.

X_i: $[x_{c_i}, y_{c_i}, \alpha_i]^T$ the 3D screw of center of mass of link i.

X: $[x_G, y_G, \phi]^T$ the 3D screw of moving platform at point G.

$\delta(\cdot)$: virtual displacement of $(\cdot)$.

Then the principle of virtual work for the manipulator can be stated as the sum of all virtual works at limbs and the moving platform should be zero.

$$\delta L^T \tau + \delta X^T \hat{F}_G + \sum_{i=1}^{4} \delta X_i \hat{F}_i = 0 \quad (25)$$

In which $\hat{F}_G = F_G + F_G^*$ is the total inertial and external wrenches exerted on the moving platform center of mass G and similarly $\hat{F}_i = F_i + F_i^*$ is that for each limb. Note that in equation 25 the actuator forces are isolated from other applied forces and torques for convenience of their derivation. Moreover, the virtual displacements in equation 25 must be compatible with the kinematic constraints imposed by the closed loop chains. Therefore, it is necessary to relate these virtual displacements to a set of independent generalized virtual

displacement, where in parallel manipulators the coordinate of the moving platform $\boldsymbol{X}$, can conveniently be chosen as the generalized coordinate. This is because the virtual displacement of limbs $\delta \boldsymbol{L}$ is related to the virtual displacement of the moving platform $\delta \boldsymbol{X}$ by the manipulator Jacobian J_M:

$$\delta \boldsymbol{L} = J_M \delta \boldsymbol{X} \tag{26}$$

Furthermore, the virtual displacement of the center of mass of limb i, $\delta \boldsymbol{X}_i$, can be related to $\delta \boldsymbol{X}$ by a similar Jacobian matrix of each limb, denoted by J_i:

$$\delta \boldsymbol{X}_i = J_i \delta \boldsymbol{X} \tag{27}$$

Substituting equations 26 and 27 into equation 25, results into:

$$\delta \boldsymbol{X}^T \left(J_M^T \boldsymbol{\tau} + \hat{\boldsymbol{F}}_G + \sum_{i=1}^{4} J_i^T \hat{\boldsymbol{F}}_i \right) = 0 \tag{28}$$

Since this is valid for any virtual displacement $\delta \boldsymbol{X}$, it follows that,

$$J_M^T \boldsymbol{\tau} + \hat{\boldsymbol{F}}_G + \sum_{i=1}^{4} J_i^T \hat{\boldsymbol{F}}_i = 0 \tag{29}$$

In general, $\mathcal{F} = J_M^T \boldsymbol{\tau}$ is the projection of the actuator forces on the moving platform, and can be uniquely determined from equation 29. Furthermore, if the manipulator has no redundancy in actuation, the Jacobian matrix, J_M, is squared and the actuator forces can be uniquely determined by $\boldsymbol{\tau} = J_M^{-T} \mathcal{F}$, provided that J_M is nonsingular. For redundant manipulators, as in our application though, there are infinitely many solution for $\boldsymbol{\tau}$ to be projected into $\mathcal{F}$. The simplest solution would be a minimum norm solution, which is found from the pseudo inverse of J_M^T, by $\boldsymbol{\tau} = J_M^{T\,\dagger} \mathcal{F}$. Other optimization techniques can be used to find the actuator forces projected from $\mathcal{F}$ which can minimize a user defined cost function. The detail of such redundancy resolution techniques are given in [11].

In order to derive the equation of motion for the manipulator by using the principle of virtual work as given in equation 29, the external and inertial generalized forces applied to the moving platform, $\hat{\boldsymbol{F}}_G$, and on each limbs $\hat{\boldsymbol{F}}_i$ is first obtained, and then the Jacobian matrices of the limbs are determined as following. The external and inertial wrench applied to the moving platform is given as:

$$\hat{\boldsymbol{F}}_G = \begin{bmatrix} \hat{\boldsymbol{f}}_G \\ \hat{\boldsymbol{n}}_G \end{bmatrix} = \begin{bmatrix} f_{D_x} - M\,\ddot{x}_G \\ f_{D_y} - M\,\ddot{y}_G \\ \tau_D - I\,\ddot{\phi} \end{bmatrix} \tag{30}$$

The external and inertial wrench applied to the limb i is determined by,

$$\hat{\boldsymbol{F}}_i = \begin{bmatrix} \hat{\boldsymbol{f}}_i \\ \hat{\boldsymbol{n}}_i \end{bmatrix} = \begin{bmatrix} -(\rho L_i)\boldsymbol{a}_{c_i} - (\rho \dot{L}_i)\boldsymbol{v}_{c_i} \\ -I_i \ddot{\alpha}_M - \dot{I}_i \dot{\alpha}_i \end{bmatrix} \tag{31}$$

In which, I_i is the moment of inertia of the limb i about its center of mass can be determined from the shape of the cables as:

$$I_i = \frac{\rho}{12} L_i^3 \qquad \longrightarrow \qquad \dot{I}_i = \frac{\rho}{4} L_i^2 \dot{L}_i \tag{32}$$

Writing equation 31 componentwise, in the following directions $[\hat{\boldsymbol{S}}_i, \hat{\boldsymbol{N}}_i, \hat{\boldsymbol{K}}]^T$, and using the velocity and acceleration of the center of mass of the limbs found in equations 23 and 24, by some manipulation we reach to:

$$\hat{\boldsymbol{F}}_i = -\frac{\rho}{2} \begin{bmatrix} L_i \ddot{L}_i - (L_i \dot{\alpha}_i)^2 + \dot{L}_i^2 \\ L_i^2 \ddot{\alpha}_i + 3 L_i \dot{L}_i \dot{\alpha}_i \\ \frac{L_i^2}{6} \left(L_i \ddot{\alpha}_i + 3 \dot{L}_i \dot{\alpha}_i \right) \end{bmatrix} \tag{33}$$

Note that the gravity force is in $-\hat{\boldsymbol{K}}$ direction and not contributing in the external forces. The next step is to derive the Jacobians. The manipulator Jacobian matrix J_M is derived earlier and is given in equation 14. The limb Jacobians J_i's are derived from the linear and angular velocity of the center of mass of the limbs, as $\hat{\boldsymbol{F}}_i$ is found in equation 33:

$$\dot{\boldsymbol{X}}_i = \begin{bmatrix} v_{C_i} \\ \dot{\alpha}_i \end{bmatrix} = \begin{bmatrix} \frac{1}{2} \dot{L}_i \hat{\boldsymbol{S}}_i \\ \frac{1}{2} L_i \dot{\alpha}_i \hat{\boldsymbol{N}}_i \\ \dot{\alpha}_i \end{bmatrix} \tag{34}$$

Substituting relations 16 and 23 into 34, the limb jacobian J_i can be derived in the same $[\hat{\boldsymbol{S}}_i, \hat{\boldsymbol{N}}_i, \hat{\boldsymbol{K}}]^T$ coordinate frame as

$$J_i = \begin{bmatrix} S_{ix}/2 & S_{iy}/2 & (E_{ix}S_{iy} - E_{iy}S_{ix})/2 \\ -S_{iy}/2 & S_{ix}/2 & (E_{ix}S_{ix} + E_{iy}S_{iy})/2 \\ -S_{iy}/L_i & S_{ix}/L_i & (E_{ix}S_{ix} + E_{iy}S_{iy})/L_i \end{bmatrix} \tag{35}$$

By Substitution of equations 14, 30, 33 and 35 into equation 29, the governing equation of motion of the manipulator is derived by some manipulation.

$$\begin{gathered} f_{D_x} - M\ddot{x}_G + \textstyle\sum_{i=1}^{4} \{(\tau_{A_i} - P_i) S_{ix} + Q_i S_{iy}\} = 0 \\ f_{D_y} - M\ddot{y}_G + \textstyle\sum_{i=1}^{4} \{(\tau_{A_i} - P_i) S_{iy} - Q_i S_{ix}\} = 0 \\ \tau_D - I\,\ddot{\phi} + \\ \textstyle\sum_{i=1}^{4} \left\{ (\tau_{A_i} - P_i)(E_{ix}S_{iy} - E_{iy}S_{ix}) - Q_i (\boldsymbol{E}_i \cdot \hat{\boldsymbol{S}}_i) \right\} = 0 \end{gathered} \tag{36}$$

in which,

$$P_i = \frac{\rho}{2} \left(L_i \ddot{L}_i - (L_i \dot{\alpha}_i)^2 + \dot{L}_i^2 \right) \tag{37}$$

$$Q_i = \frac{\rho}{3} \left(L_i^2 \ddot{\alpha}_i + 3 L_i \dot{L}_i \dot{\alpha}_i \right). \tag{38}$$

V. Implementation of The Formulations

Assume that the desired trajectory of the manipulator is given, and the actuator forces required to generate such trajectories, in presence of disturbance forces are to be determined. Due to the implicit nature of dynamic equations, as it is illustrated in figure 5, the dynamic formulation is implemented in the following sequence.

The first step of dynamic equation implementation is to solve the inverse kinematics of the manipulator and to find $\boldsymbol{L}(t)$ and $\boldsymbol{\alpha}(t)$, using equations 8, 9, respectively. Then the manipulator Jacobian matrix J_M is calculated by the equation 14. By this means $\dot{\boldsymbol{L}}(t)$ and $\dot{\boldsymbol{\alpha}}(t)$, are calculated. Next the accelerations are evaluated using the acceleration analysis equations 20 and 22. Finally, the inertial forces, namely, P_i and Q_i are

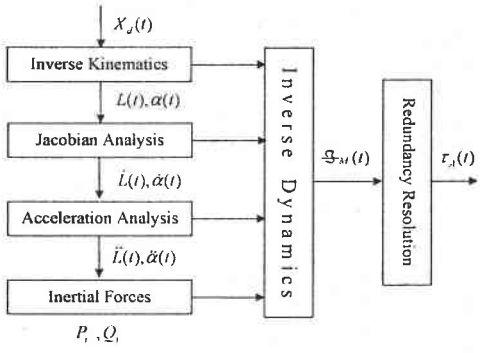

Fig. 5. Flowchart of inverse dynamics implementation sequence.

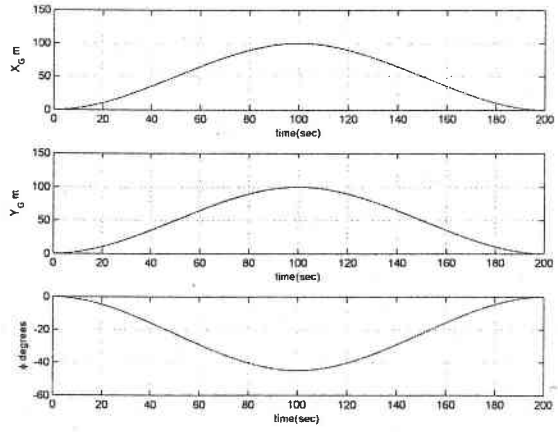

Fig. 6. The trajectory of the redundant manipulator

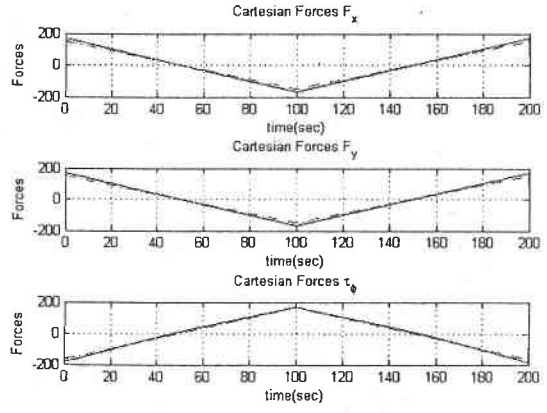

Fig. 7. The cartesian forces of the manipulator, $\mathcal{F}_M$; The total force (solid), neglecting limbs inertia (dashed)

computed from equations 37 and 38, and is substituted in the governing inverse dynamic equations of the manipulator. In order to implement redundancy resolution block, let us denote the resulting cartesian force applied to the moving platform $\mathcal{F}$, as defined in equation 29. In this definition $\mathcal{F}$ is the resulting cartesian forces applied to the manipulator, which is calculated from the summation of all inertial, and external forces *excluding the actuator torques* τ_A in the dynamic equations 36. Hence, $\mathcal{F} = J_M^T \tau_A$ is the projection of the actuator forces on the moving platform, and can be uniquely determined from the dynamic equations by excluding the actuator forces from the dynamic equations. If the manipulator has no redundancy in actuation, the Jacobian matrix, J_M, is square and the actuator forces can be uniquely determined by $\tau_A = J_M^{-T} \mathcal{F}$, provided that J_M is nonsingular. For redundant manipulators, however, there are infinity many solution for τ_A to be projected into $\mathcal{F}$. The simplest redundancy resolution would be a minimum norm solution, which is found from the pseudo inverse of J_M^T, by $\tau_A = J_M^{T\dagger} \mathcal{F}$. This solution is implemented in the simulations presented in this section. Other optimization techniques are used to find the actuator forces projected from $\mathcal{F}$ subject to more detailed manipulator constraints, whose details are reported in [11].

The dynamics of the manipulator is simulated for two cases. In first set of simulation results, the inverse dynamic solution is computed in absence of disturbance forces $F_D[f_{D_x}, f_{D_y}, \tau_D]^T = 0$. The simulation results are illustrated in figures 7 and 8. A typical third order polynomial trajectories for the manipulator is considered in these simulation, which is depicted in figure 6. The cartesian forces at moving platform, $\mathcal{F}_M = [\mathcal{F}_X, \mathcal{F}_Y, \mathcal{F}_\phi]^T$, are illustrated in solid line in figure 7. As it is seen in this figure, the cartesian forces have similar pattern to the desired trajectory accelerations, which are linear for the cubic trajectories. In order to compare the contribution of the moving platform inertia compared to that of the limb inertial terms, the moving platform inertia forces are depicted in dashed line in figure 7. As it is seen in this figure the effect of the limb inertia forces are about %10 of the total for such trajectories. Similarly, the actuator forces for the manipulator with the indication of moving platform inertia contributions are illustrated in figure 8. It is observed that since the manipulator moves in positive x and y directions, the actuator forces of first and third limbs are dominant.

In the second set of simulations, the effect of disturbance forces acting on the system is analyzed. A set of experimental disturbance forces are considered in this study to be present in the simulations. The disturbance forces, which are due to the wind turbulence, are measured in the one-third scale prototype of the multi-tethered aerostat subsystem [6], which is implemented in Penticton. The horizontal measured forces are scaled–up by a factor of 27 and are applied on the dynamic simulations, in order to replicate the behavior of the full size system. The exerted disturbance forces on the manipulator are given in dotted line in figure 9. The cartesian and actuator forces of the manipulator in presence of such disturbance is depicted in figures 9, and 10, respectively. As it is seen in these figures the contribution of the disturbance force into the total cartesian forces on the manipulator is dominant. Comparing the values of forces in figures 7 and 9, it is observed that the total inertial forces contribute about %10 of the total forces, for such typical disturbances. Noting that the limb dynamics contributes only in %10 of inertial forces, it can be neglected in the full simulation of the system in presence of external disturbances.

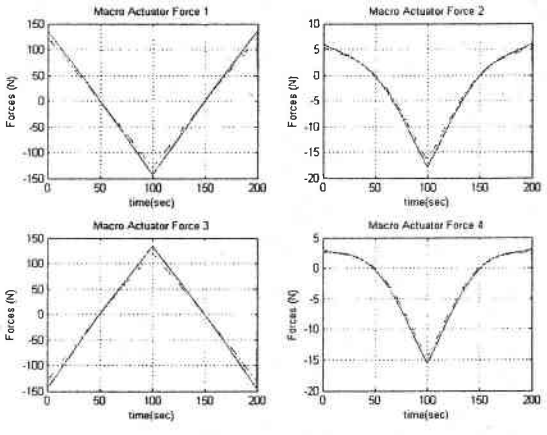

Fig. 8. The actuator forces of the manipulator, τ_A; The total force (solid), neglecting limbs inertia (dashed)

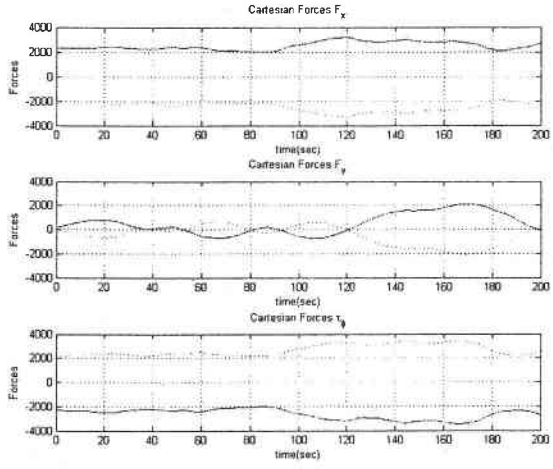

Fig. 9. The cartesian forces of the manipulator $\mathcal{F}_M$, in presence of empirical disturbance $\boldsymbol{F}_d$.

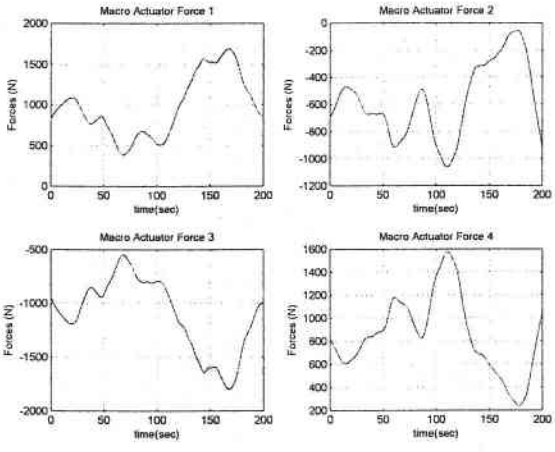

Fig. 10. The actuator forces of the manipulator τ_A, in presence of empirical disturbance $\boldsymbol{F}_d$.

VI. Conclusions

In this paper the kinematic and dynamic analysis of a redundantly actuated parallel manipulator is studied in detail. The analyzed manipulator is a planar version adopted from the structure of Large Adaptive Reflector (LAR), the Canadian design of next generation giant radio telescopes. In the LAR design the telescope receiver package is supported by a tension structure consisting of multiple long tethers and a helium filled aerostat. In the positioning structure of the receiver a redundantly actuated cable-driven parallel manipulators is used which experiences a 6DOF motion in the space. The planar structure used in this paper, is a simplified version of LAR design, in which the two important feature of the main mechanism, namely the actuator redundancy, and cable driven actuation are preserved in a planar structure. This structure is composed of a 3DOF parallel redundant manipulator actuated by cables. A thorough analysis on the kinematics and dynamics of the described parallel manipulator has been developed and some closed loop control topologies are proposed and simulated for this system. In this paper the kinematic and dynamic analysis of this system is presented. It is shown that unique closed form solution to the inverse kinematic problem of such structure exists. Moreover, The jacobian and acceleration analysis for the manipulator is reported. Next, the dynamic equation of motion of the redundant manipulator is derived using the principle of virtual work. Then, the dynamic equations of the system is used in two sets of simulations. First, the required actuator torques required to generate a predefined trajectory is computed. It is shown that for a typical trajectory, the limb inertial forces contributes only in %10 of the dynamical forces. Moreover the actuator forces are simulated in the presence of experimentally measured disturbance forces. It is shown that in this case the total inertial forces contribute in only %10 of the external forces.

Acknowledgements

The authors gratefully acknowledge the financial support received from the K.N. Toosi University of Technology, and PBEEE Quebec Visiting Scientist Award, and the Natural Sciences and Engineering Research Council of Canada, which makes this research possible.

References

[1] B. Carlson, L. Bauwens, L. Belototski, E. Cannon, Y. Deng, P. Dewdney, J. Fitzsimmons, D. Halliday, K. Krschner, G. Lachapelle, D. Lo, P. Mousavi, M. Nahon, L. Shafai, S. Stiemer, R. Taylor, and B. Veidt. The large adaptive reflector: A 200-m diameter, wideband, cm-wave radio telescope. In *Radio Telescopes-Proc. of SPIE Meeting 4015*, pages 33–44, Bellingham,WA, 2000.

[2] Hui Cheng, Yiu-Kuen Yiu, and Zexiang Li. Dynamics and control of redundantly actuated parallel manipulators. *IEEE/ASME Transactions on Mechatronics*, 8(4):483–491, Dec. 2003.

[3] N. Dasgupta and T.S. Mruthyunjaya. A newton-euler formulation for the inverse dynamics of the stewart platform manipulator. *Mechanism and Machine Theory*, 33(8):1135–52, 1998.

[4] C. Gosselin. Parallel computational algorithms for the kinematics and dynamics of planar and spatial parallel manipulators. *Trans. ASME Journal of Dynamic Systems, Measurement and Control*, 118(1):22–28, 1996.

[5] M.V. Ivashina, A. Van Ardenne, J.D. Bregman, J.G.B. de Vaate, and M. van Veelen. Activities for the square kilometer array (ska) in europe. In *Int. Conf. Antenna Theory and Techniques*, pages 633–636, Sept. 2003.

[6] C. Lambert, A. Saunders, C. Crawford, and M. Nahon. Design of a one-third scale multi-tethered aerostat system for precise positioning of a radio telescope receiver. In *CASI Flight Mechanics and Operations Symposium, Montreal*, 2003.

[7] G. Lebret, K. Liu, and F.L. Lewis. Dynamic analysis and control of a stewart platform manipulator. *Journal of Robotic Systems*, 10(5):629–655, July 1993.

[8] J. McPhee, P. Shi, and J.C. Piedboeuf. Dynamics of multibody systems using virtual work and symbolic programming. *Mathematical and Computer Modelling of Dynamical Systems*, 8(2):137–155, June 2002.

[9] C.C. Nguyen and F.J Pooran. Dynamic analysis of a 6 DOF CKCM robot end-effector for dual-arm telerobot systems. *Robotics and Autonomous Systems*, 5(4):377–394, Dec. 1989.

[10] H.D. Taghirad and M. Nahon. Kinematic analysis of a macro–micro redundantly actuated parallel manipulator. Submitted to Advanced Robotics, July 2006.

[11] H.D. Taghirad and M. Nahon. Redundancy resolution and inverse dynamics control of a macro–micro redundantly actuated parallel manipulator. Submitted to International Journal of Robotics Systems, Feb. 2007.

[12] Jiegao Wang and C.M. Gosselin. A new approach for the dynamic analysis of parallel manipulators. *Multibody System Dynamics*, 2(3):317–334, Sept. 1998.